

# THE TRANSFER FUNCTION ANALYSIS OF VARIOUS SCHEMES FOR THE TWO-DIMENSIONAL SHALLOW-WATER EQUATIONS

B. NETA and C. L. DEVITO

Department of Mathematics, Naval Postgraduate School, Monterey, CA 93943, U.S.A.

**Abstract**—In this paper various finite difference and finite element approximations to the linearized two-dimensional shallow-water equations are analyzed. This analysis complements previous results for the one-dimensional case.

## 1. INTRODUCTION

This paper can be viewed as an outgrowth of Schoenstadt's results [1]. The transfer function analysis given there is extended to the two-dimensional linearized shallow-water system.

In the next section we discuss the exact solution of the shallow-water equations with no mean flow. We obtain an expression for the phase speed and both group velocities. Section 3 will be devoted to various finite element and finite difference approximations to the system. The phase speed and group velocities of the schemes will be compared to the results of Section 2. The rectangular bilinear elements and the isosceles triangular linear elements are at least as good as the staggered fourth-order C-scheme.

## 2. SHALLOW-WATER EQUATIONS

The equations to be analyzed are the two-dimensional linearized shallow-water equations, with no mean flow:

$$\left. \begin{aligned} \frac{\partial u}{\partial t} - fv + g \frac{\partial h}{\partial x} &= 0 \\ \frac{\partial v}{\partial t} + fu + g \frac{\partial h}{\partial y} &= 0 \\ \frac{\partial h}{\partial t} + H \left( \frac{\partial u}{\partial x} + \frac{\partial v}{\partial y} \right) &= 0, \end{aligned} \right\} \quad (1)$$

where  $u, v$  denote the perturbation velocity components in the  $x, y$  direction, respectively;  $H, h$  denote the mean and perturbed heights of the free surface, respectively; and  $g, f$  denote the gravitational and Coriolis parameters, respectively. This model is important in the study of geostrophic adjustment in meteorology. This process was studied from several approaches by Rossby [2], Cahn [3], Winninghoff [4], Blumen [5], Arakawa and Lamb [6], Schoenstadt [1, 7] and Neta and Navon [8]. The dispersive wave nature of equations (1) is the primary mechanism by which errors in the initial data eventually spread out over the domain of interest.

Generalizing the results of Schoenstadt [1, 7], let

$$\tilde{u}(k, l, t) = \iint u(x, y, t) e^{-ikx+ly} dx dy \quad (2)$$

be the Fourier transform of  $u$ , and similarly for the other variables, then equations (1) reduce to

$$\left. \begin{aligned} \frac{d\tilde{u}}{dt} - f\tilde{v} + ikg\tilde{h} &= 0 \\ \frac{d\tilde{v}}{dt} + f\tilde{u} + ilg\tilde{h} &= 0 \\ \frac{d\tilde{h}}{dt} + ikH\tilde{u} + ilH\tilde{v} &= 0, \end{aligned} \right\} \quad (3)$$

together with the initial conditions

$$\tilde{A}_0 = \tilde{A}(k, l, 0) = \int \int A(x, y, 0) e^{-i(kx+ly)} dx dy, \quad (4)$$

where  $A$  is  $u$ ,  $v$  or  $h$ . The system (3) is a set of constant coefficient ordinary differential equations whose solution is given by

$$\tilde{u} = A_1 + B_1 e^{ivt} + C_1 e^{-ivt}, \quad (5a)$$

$$\tilde{v} = A_2 + B_2 e^{ivt} + C_2 e^{-ivt}, \quad (5b)$$

$$\tilde{h} = A_3 + B_3 e^{ivt} + C_3 e^{-ivt}, \quad (5c)$$

where

$$v = \sqrt{1 + \lambda^2(k^2 + l^2)}; \quad (6)$$

$\lambda$  is the Rossby radius given by

$$\lambda = \sqrt{gH/f}. \quad (7)$$

A lengthy algebraic manipulation shows that

$$A_1 = -\frac{l}{k} A_2, \quad (8a)$$

$$A_3 = -i \frac{f}{kg} A_2, \quad (8b)$$

$$B_2 = \frac{ivl - fk}{ivk + fl} B_1, \quad (8c)$$

$$B_3 = -\frac{i(k^2 + l^2)H}{ivk + fl} B_1, \quad (8d)$$

$$C_2 = \frac{ivl + fk}{ivk - fl} C_1 \quad (8e)$$

and

$$C_3 = \frac{i(k^2 + l^2)H}{ivk - fl} C_1. \quad (8f)$$

Notice that if  $l = 0$  one obtains the solution for the one-dimensional case given by Schoenstadt [1]. The free parameters  $A_2$ ,  $B_1$ ,  $C_1$  can be specified by the initial conditions. One can show by using any symbolic manipulator (REDUCE [9] is used in this case) that

$$\tilde{u} = \tilde{u}_0 + \frac{1}{v^2} \left\{ (f^2 + gHk^2)\tilde{u}_0 + gHkl\tilde{v}_0 + igfl\tilde{h}_0 \right\} \cos vt + \frac{1}{v} \left\{ f\tilde{v}_0 - ikg\tilde{h}_0 \right\} \sin vt, \quad (9)$$

$$\tilde{v} = \tilde{v}_0 + \frac{1}{v^2} \left\{ gHkl\tilde{u}_0 + (f^2 + gHl^2)\tilde{v}_0 - ifkg\tilde{h}_0 \right\} \cos vt - \frac{1}{v} \left\{ f\tilde{u}_0 + iglh_0 \right\} \sin vt, \quad (10)$$

$$\tilde{h} = \tilde{h}_s + \frac{1}{v^2} \left\{ -iHf\tilde{u}_0 + iHfk\tilde{v}_0 + gH(k^2 + l^2)\tilde{h}_0 \right\} \cos vt - \frac{1}{v} \left\{ iHk\tilde{u}_0 + iHl\tilde{v}_0 \right\} \sin vt, \quad (11)$$

where the steady-state solution is

$$\tilde{u}_s = \frac{1}{v^2} \left\{ gHl^2\tilde{u}_0 - gHkl\tilde{v}_0 - igf\tilde{h}_0 \right\}, \quad (12a)$$

$$\tilde{v}_s = \frac{1}{v^2} \left\{ -gHkl\tilde{u}_0 + gHk^2\tilde{v}_0 + igfk\tilde{h}_0 \right\}, \quad (12b)$$

$$\tilde{h}_s = \frac{1}{v^2} \left\{ iHf\tilde{u}_0 - iHfk\tilde{v}_0 + f^2\tilde{h}_0 \right\}. \quad (12c)$$

Notice that  $\tilde{u}_s$  and  $\tilde{v}_s$  satisfy the geostrophic relations

$$\tilde{u}_s = -i \frac{lg}{f} \tilde{h}_s \quad (13a)$$

and

$$\tilde{v}_s = i \frac{kg}{f} \tilde{h}_s. \quad (13b)$$

Note also that equation (12c) agrees with the steady solution given, for example, by Washington [10].

An examination of equations (9)–(11) shows that the amplitude distortion in the system is governed by one of the six factors  $1/v$ ,  $k/v$ ,  $l/v$ ,  $k/v^2$ ,  $l/v^2$ ,  $kl/v^2$ ; or the square of one of these. The amplitude response contours are shown in Fig. 1. Note that the last three are the product of two of the first three.

The phase speed and the zonal and meridional group velocities are shown in Fig. 2. Recall that the group velocities govern the rate at which energy propagates. The formulae are

$$\frac{\partial v}{\partial k} = f \frac{k\lambda^2}{\sqrt{1 + \lambda^2(k^2 + l^2)}} \quad (14)$$

and

$$\frac{\partial v}{\partial l} = f \frac{l\lambda^2}{\sqrt{1 + \lambda^2(k^2 + l^2)}}. \quad (14)$$

### 3. QUASI-DISCRETE FINITE DIFFERENCE AND FINITE ELEMENT METHODS

In this section, we analyze several finite difference and finite element methods discretizing the spatial derivatives. The time derivatives are not discretized. The finite difference schemes considered are of order 2 and 4 and denoted by A, B, C and D, as in other works [1, 4, 6 etc.]. We also include the linear finite elements on isosceles triangles and bilinear rectangular elements. Other triangulations have been shown to be inferior to these two [11, 12].

The quasi-discrete system in all these cases is of the form

$$\left. \begin{aligned} \alpha \frac{\partial \tilde{u}}{\partial t} - \beta f \tilde{v} + i\gamma_1 g \tilde{h} &= 0 \\ \alpha \frac{\partial \tilde{v}}{\partial t} + \beta f \tilde{u} + i\gamma_2 g \tilde{h} &= 0 \\ \alpha \frac{\partial \tilde{h}}{\partial t} + iH(\gamma_1 \tilde{u} + \gamma_2 \tilde{v}) &= 0. \end{aligned} \right\} \quad (14)$$

The parameters  $\alpha$ ,  $\beta$ ,  $\gamma_1$ ,  $\gamma_2$  depend on the method and are listed in Tables 1–3.

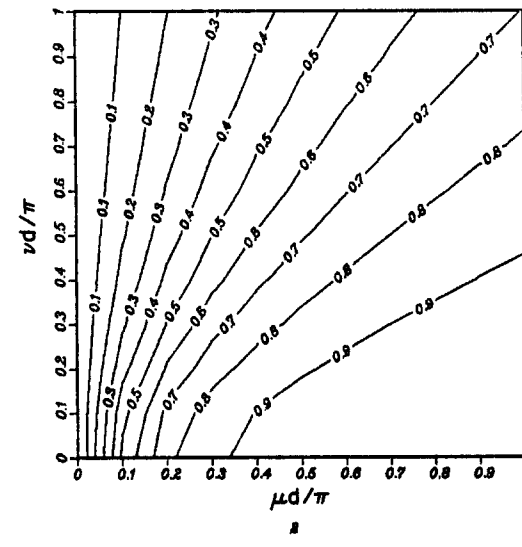
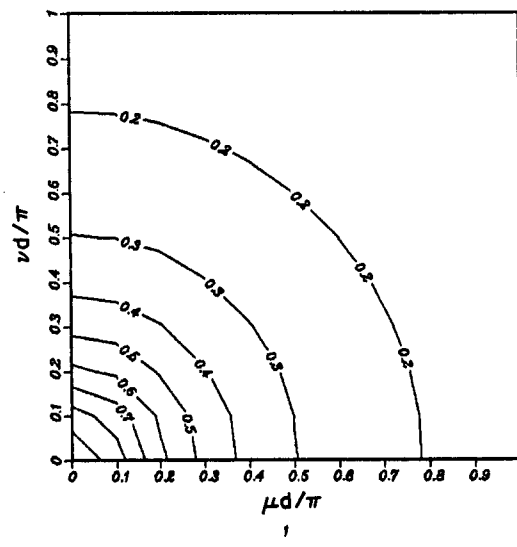
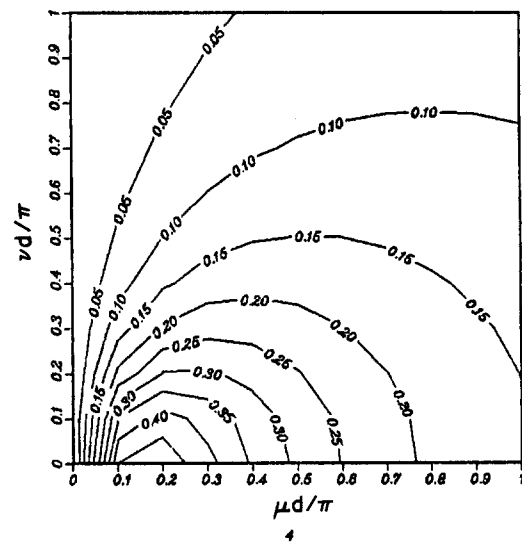
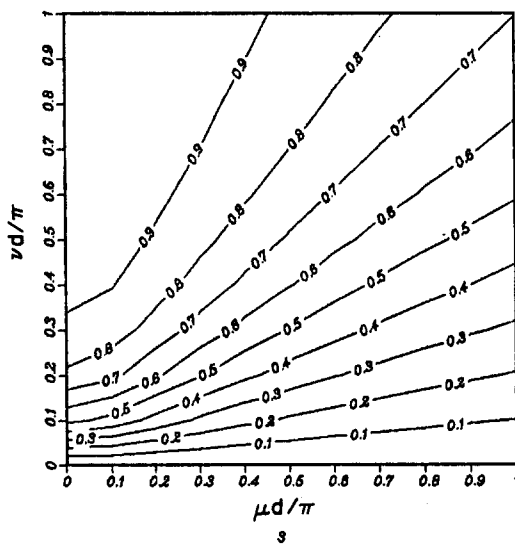
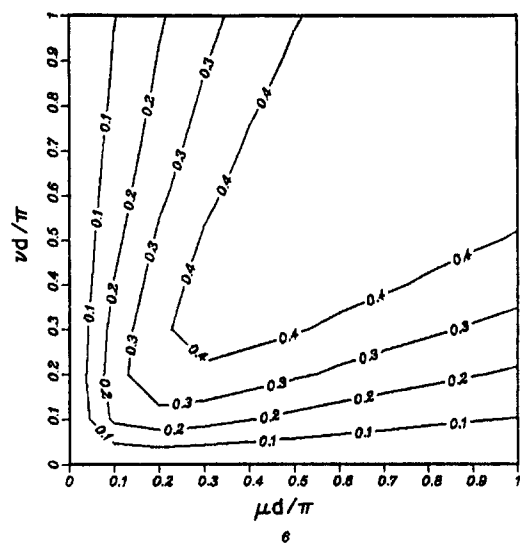
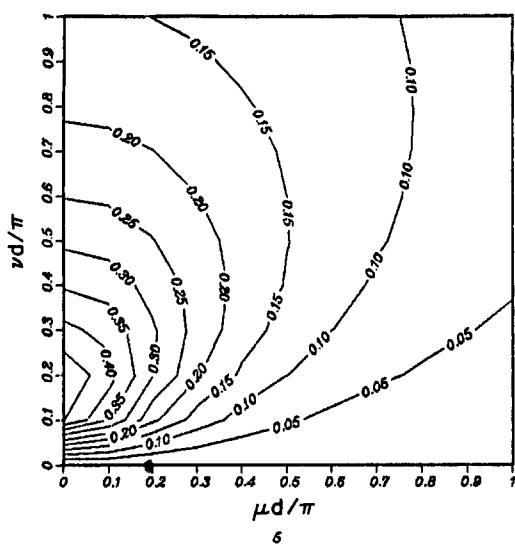


Fig. 1

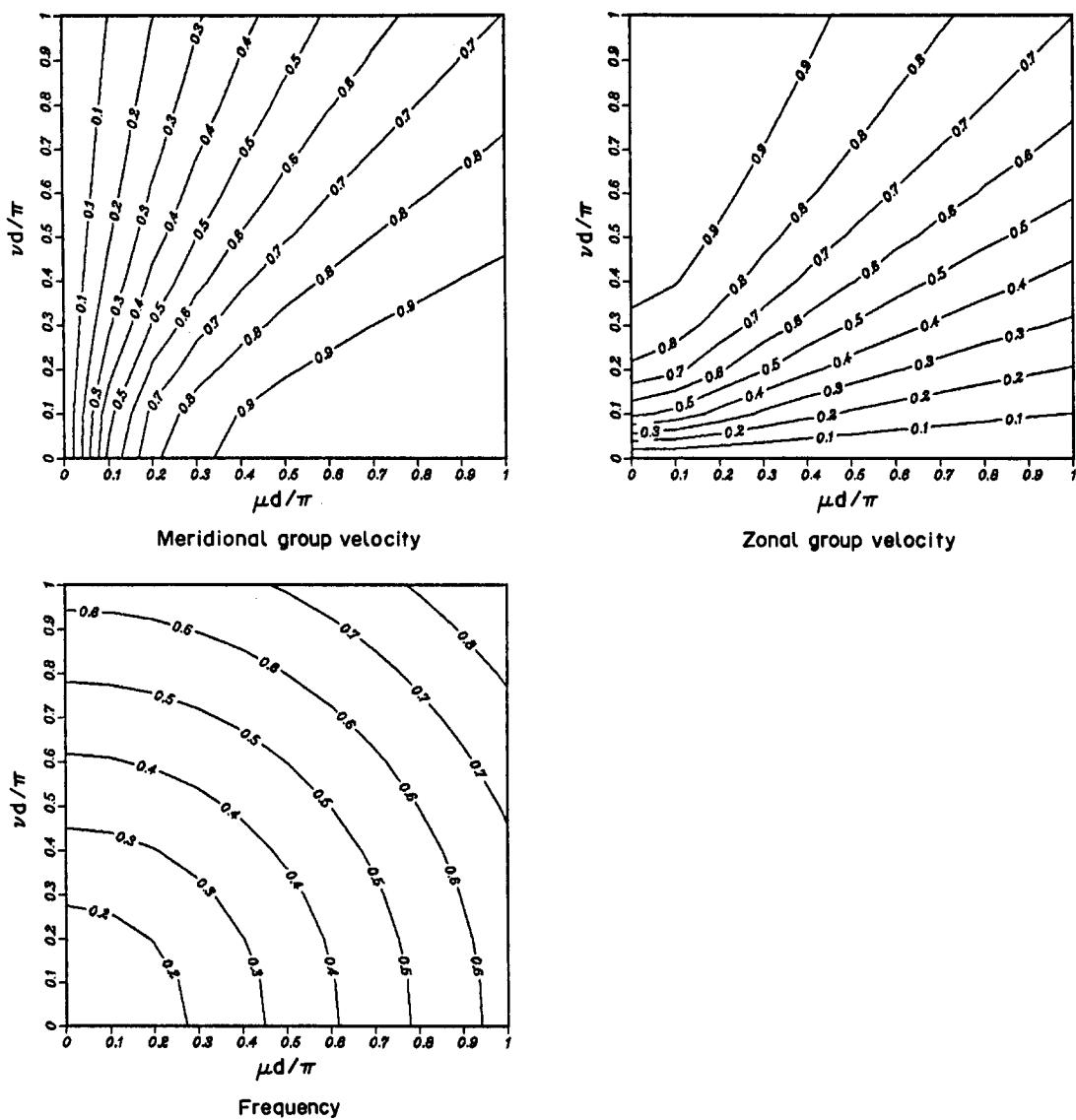


Fig. 2

Equations (14) can be solved in the same way and one obtains

$$\begin{aligned} \tilde{u} = \tilde{u}_s + \frac{1}{\alpha^2 \nu^2} \left\{ (\beta^2 f^2 + gH\gamma_1^2) \tilde{u}_0 + gH\gamma_1 \gamma_2 \tilde{v}_0 + ig\beta f \gamma_2 \tilde{h}_0 \right\} \cos \nu at \\ + \frac{1}{\alpha \nu} \left\{ \beta f \tilde{v}_0 - ig\gamma_1 \tilde{h}_0 \right\} \sin \alpha vt, \quad (15) \end{aligned}$$

$$\begin{aligned} \tilde{v} = \tilde{v}_s + \frac{1}{\alpha^2 \nu^2} \left\{ gH\gamma_1 \gamma_2 \tilde{u}_0 + (\beta^2 f^2 + gH\gamma_2^2) \tilde{v}_0 - if\beta g \gamma_1 \tilde{h}_0 \right\} \cos \nu at \\ - \frac{1}{\alpha \nu} \left\{ \beta f \tilde{u}_0 + ig\gamma_2 \tilde{h}_0 \right\} \sin \alpha vt, \quad (16) \end{aligned}$$

$$\begin{aligned} \tilde{h} = \tilde{h}_s + \frac{1}{\alpha^2 \nu^2} \left\{ -iHf\beta \gamma_2 \tilde{u}_0 + iHf\beta \gamma_1 \tilde{v}_0 + gH(\gamma_1^2 + \gamma_2^2) \tilde{h}_0 \right\} \cos \nu at \\ - \frac{1}{\alpha \nu} \left\{ iH\gamma_1 \tilde{u}_0 + iH\gamma_2 \tilde{v}_0 \right\} \sin \alpha vt, \quad (17) \end{aligned}$$

Table 1. Filter weights for second-order finite differences

Scheme	$\alpha$	$\beta$	$\gamma_1$	$\gamma_2$
A2	1	1	$\frac{\sin kd}{d}$	$\frac{\sin ld}{d}$
B2	1	1	$\frac{\sin k \frac{d}{2}}{d/2} \cos l \frac{d}{2}$	$\frac{\sin l \frac{d}{2}}{d/2} \cos k \frac{d}{2}$
C2	1	$\cos k \frac{d}{2} \cos l \frac{d}{2}$	$\frac{\sin k \frac{d}{2}}{d/2}$	$\frac{\sin l \frac{d}{2}}{d/2}$
D2	1	$\cos k \frac{d}{2} \cos l \frac{d}{2}$	$\frac{\sin kd}{d} \cos l \frac{d}{2}$	$\frac{\sin ld}{d} \cos k \frac{d}{2}$

where the steady-state solution is

$$\tilde{u}_s = \frac{1}{\alpha^2 v^2} \{ gH\gamma_2^2 \tilde{u}_0 - gH\gamma_1\gamma_2 \tilde{v}_0 - igf\beta\gamma_2 \tilde{h}_0 \}, \quad (18a)$$

$$\tilde{v}_s = \frac{1}{\alpha^2 v^2} \{ -gH\gamma_1\gamma_2 \tilde{u}_0 + gH\gamma_1^2 \tilde{v}_0 + igf\beta\gamma_1 \tilde{h}_0 \}, \quad (18b)$$

$$\tilde{h}_s = \frac{1}{\alpha^2 v^2} \{ iHf\beta\gamma_2 \tilde{u}_0 - iHf\beta\gamma_1 \tilde{v}_0 + \beta^2 f^2 \tilde{h}_0 \}; \quad (18c)$$

and

$$\alpha v = f \sqrt{\beta^2 + \lambda^2 (\gamma_1^2 + \gamma_2^2)}. \quad (19)$$

Note that in obtaining equations (15)–(18) one just replaces  $f, k, l, v$  by  $\beta f, \gamma_1, \gamma_2, \alpha v$ , respectively.

The filter coefficients are replaced by

$$\frac{\beta}{\alpha v}, \quad \frac{\gamma_1}{\alpha v}, \quad \frac{\gamma_2}{\alpha v}, \quad \frac{\beta\gamma_1}{\alpha^2 v^2}, \quad \frac{\beta\gamma_2}{\alpha^2 v^2}, \quad \frac{\gamma_1\gamma_2}{\alpha^2 v^2},$$

or the square of one of these.

In Figs 3–12 we plot the contours of these amplitudes relative to the exact ones. In each of these figures we have six contours for the six filter coefficients. Analysis of the contours show that the

Table 2. Filter weights for fourth-order finite differences

Scheme	$\alpha$	$\beta$	$\gamma_1$	$\gamma_2$
A4	1	1	$\frac{8 \sin kd - \sin 2kd}{6d}$	$\frac{8 \sin ld - \sin 2ld}{6d}$
B4	1	1	$\frac{-\sin \frac{1}{2}kd + 27 \sin \frac{1}{2}kd}{12d} \cos l \frac{d}{2}$	$\frac{-\sin \frac{1}{2}ld + 27 \sin \frac{1}{2}ld}{12d} \cos k \frac{d}{2}$
C4	1	$\cos k \frac{d}{2} \cos l \frac{d}{2}$	$\frac{-\sin \frac{1}{2}kd + 27 \sin \frac{1}{2}kd}{12d}$	$\frac{-\sin \frac{1}{2}ld + 27 \sin \frac{1}{2}ld}{12d}$
D4	1	$\cos k \frac{d}{2} \cos l \frac{d}{2}$	$\frac{8 \sin kd - \sin 2kd}{6d} \cos l \frac{d}{2}$	$\frac{8 \sin ld - \sin 2ld}{6d} \cos k \frac{d}{2}$

Table 3. Filter weights for finite elements

Scheme	$\alpha = \beta$	$\gamma_1$	$\gamma_2$
FET	$\frac{3 + \cos kd + 2 \cos k \frac{d}{2} \cos ld}{6}$	$\frac{2 \left( \sin kd + \sin k \frac{d}{2} \cos ld \right)}{3d}$	$\cos k \frac{d \sin ld}{2}$
FER	$\frac{(2 + \cos kd)(2 + \cos ld)}{9}$	$\frac{2 + \cos ld \sin kd}{3d}$	$\frac{2 + \cos kd \sin ld}{3d}$

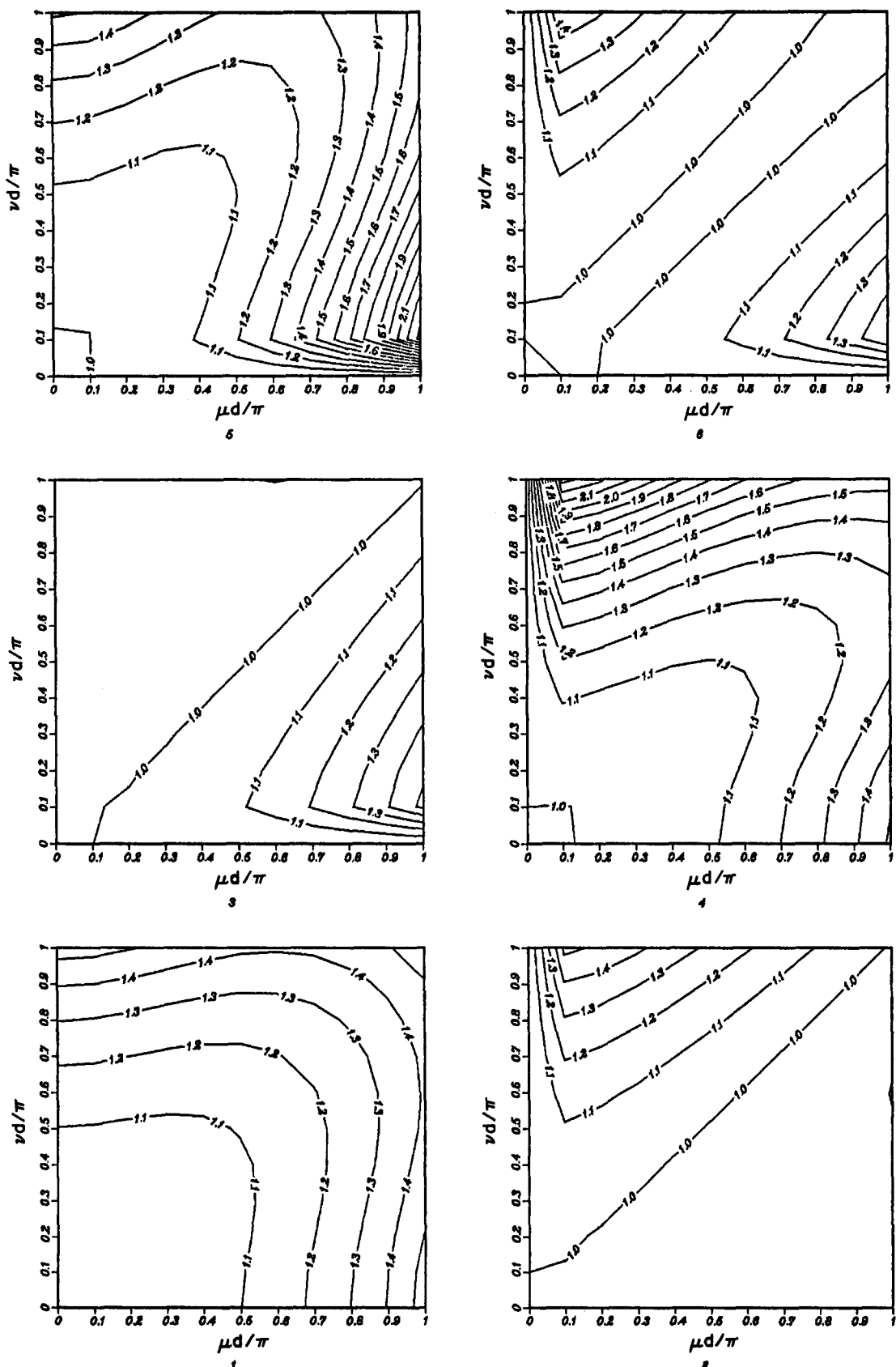


Fig. 3. Scheme A2.

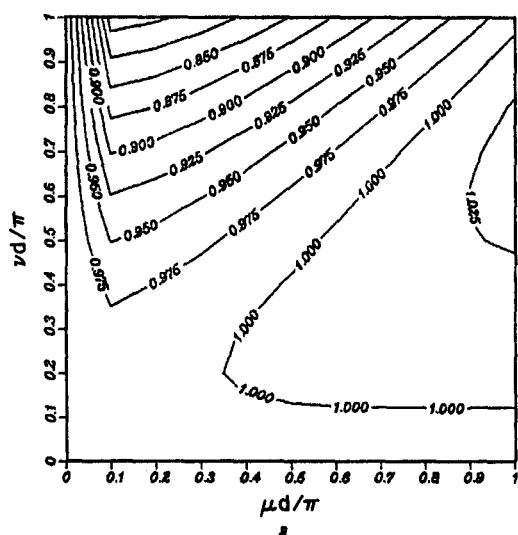
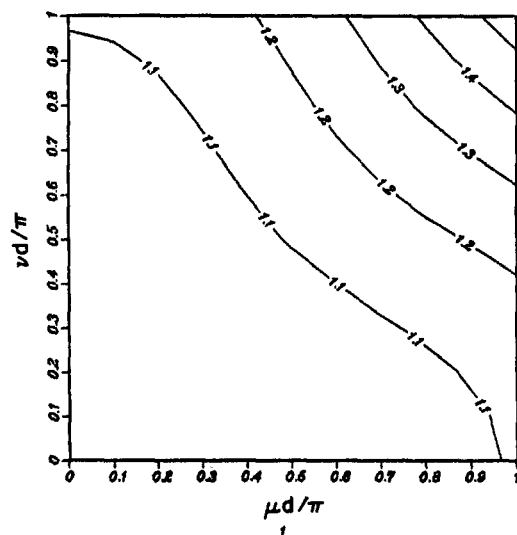
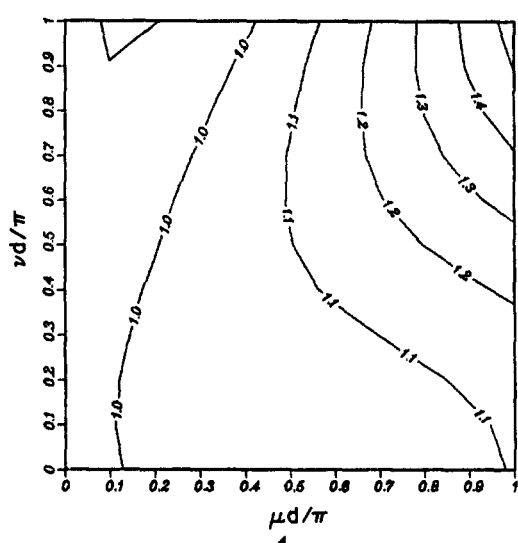
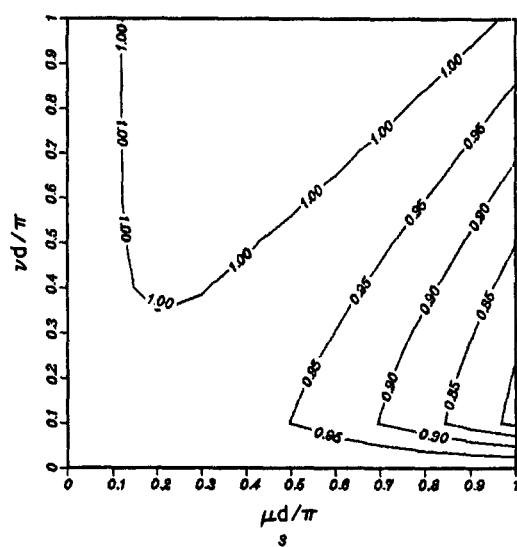
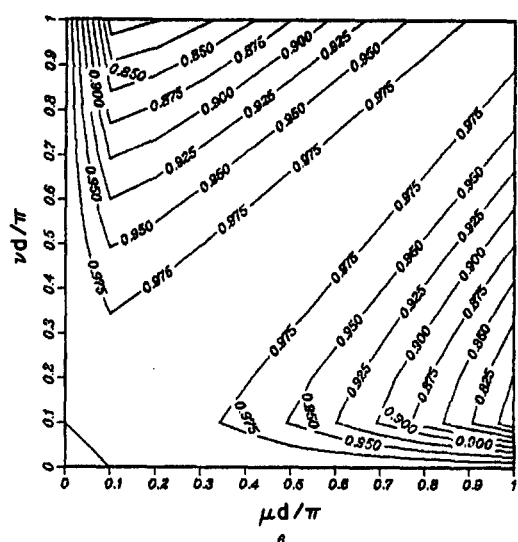
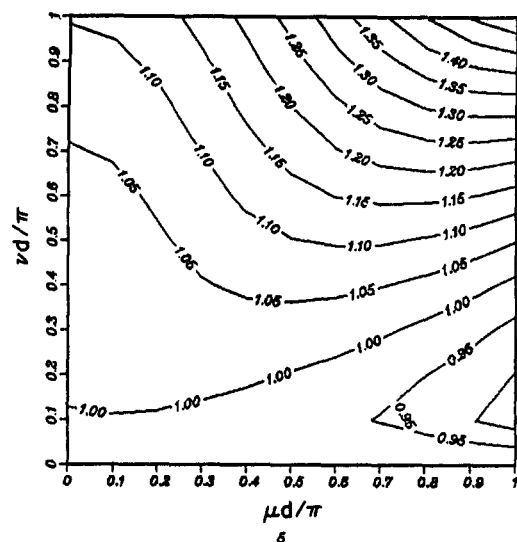


Fig. 4. Scheme B2.

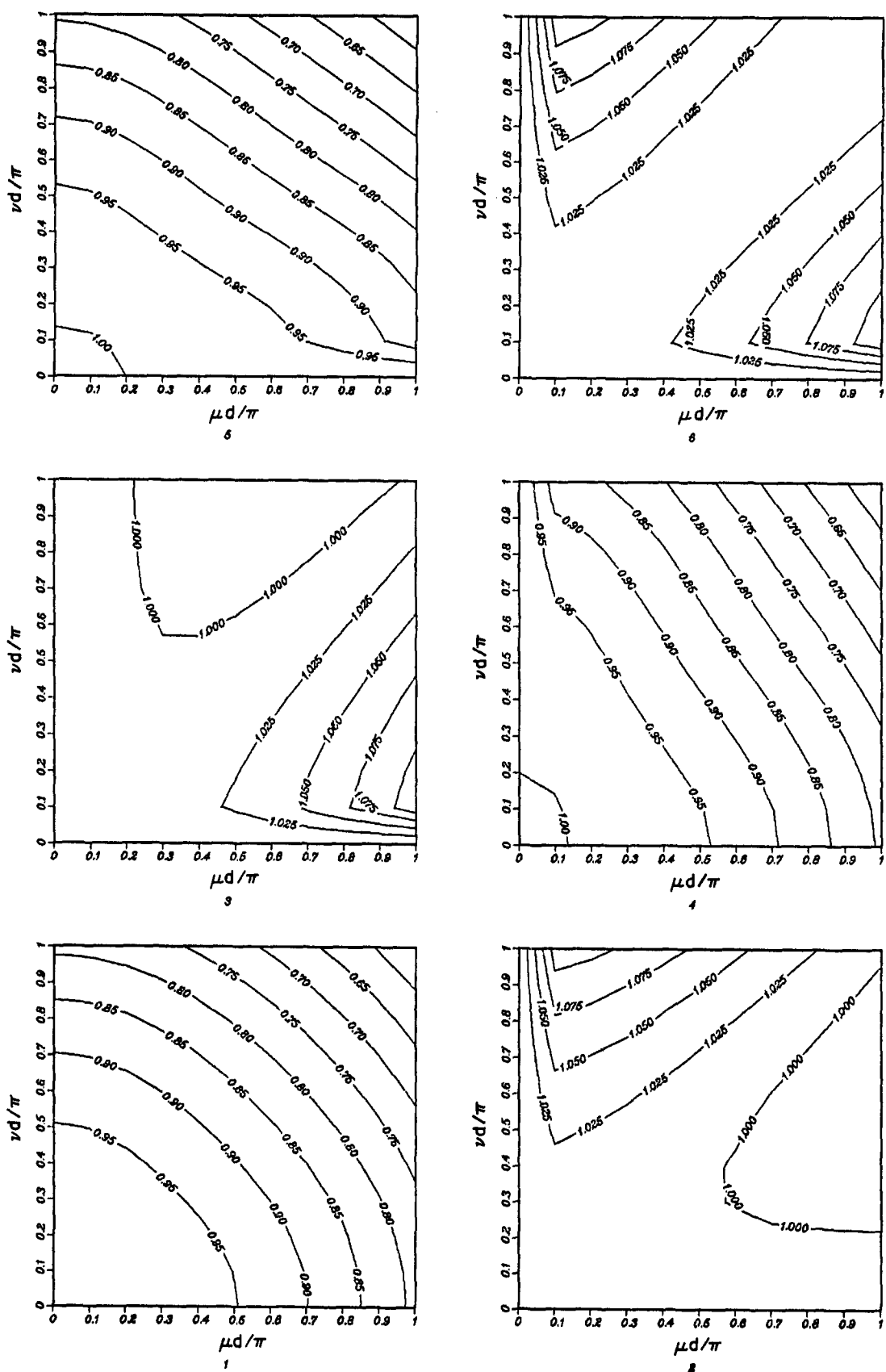


Fig. 5. Scheme C2.

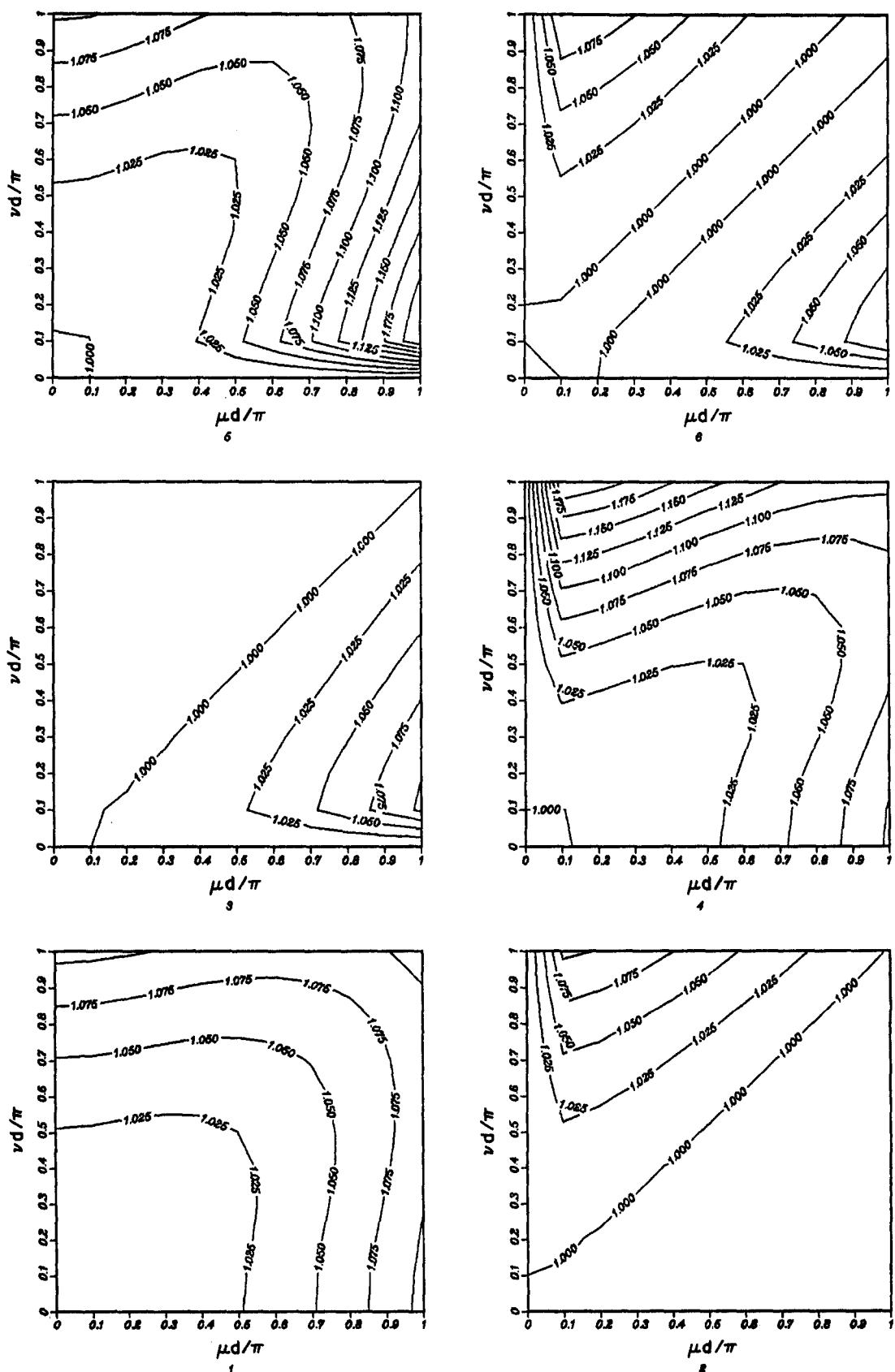


Fig. 6. Scheme D2.

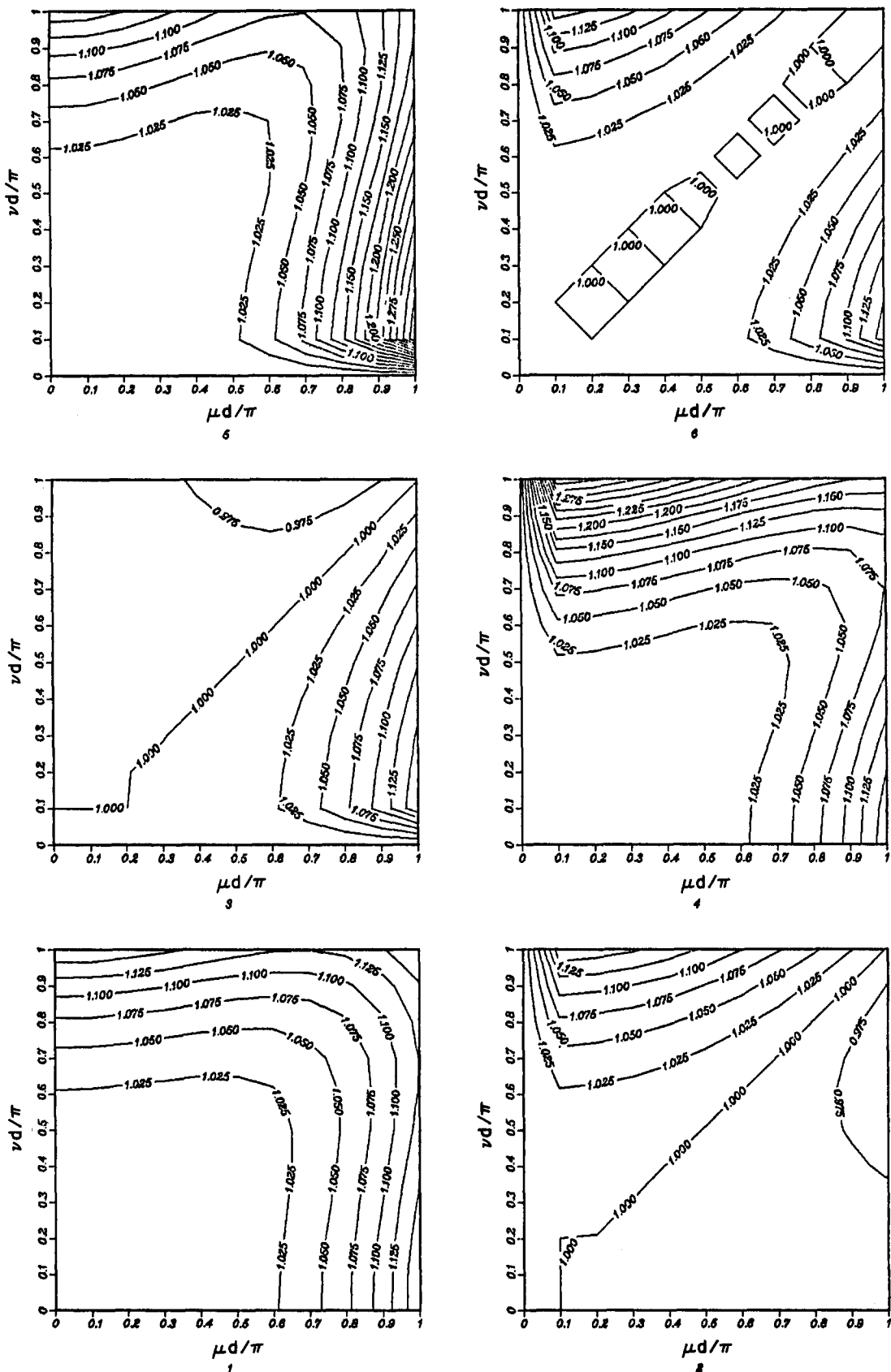


Fig. 7. Scheme A4.

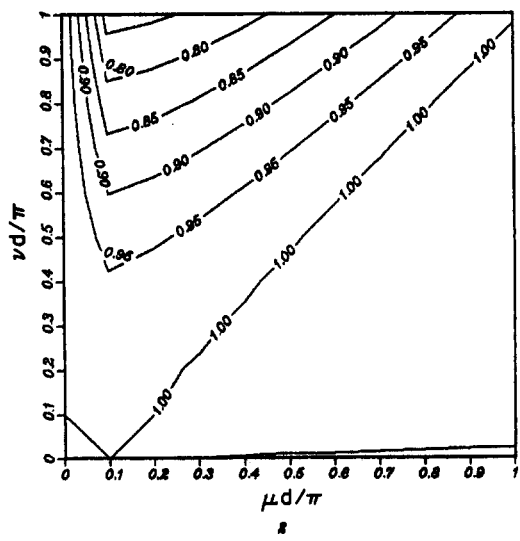
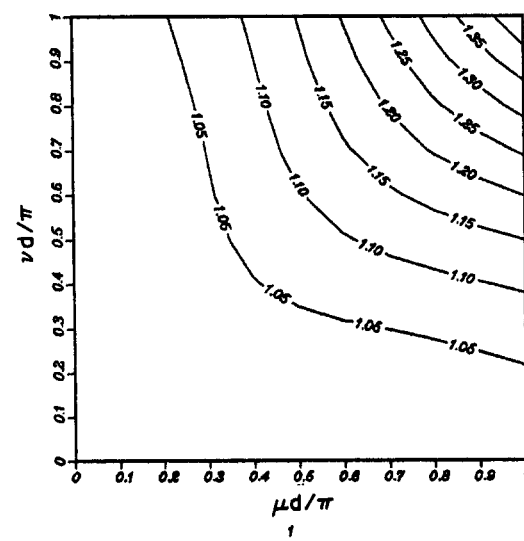
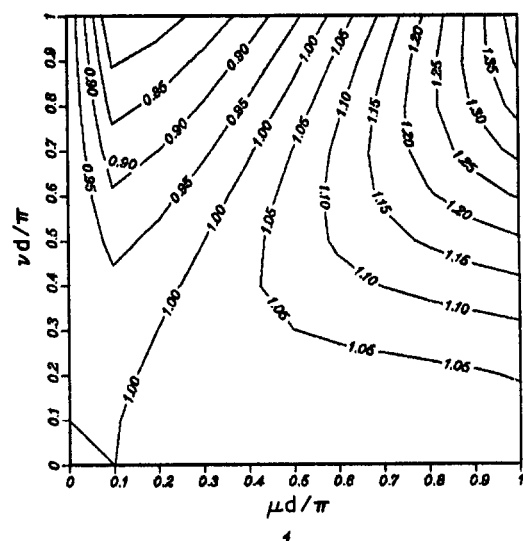
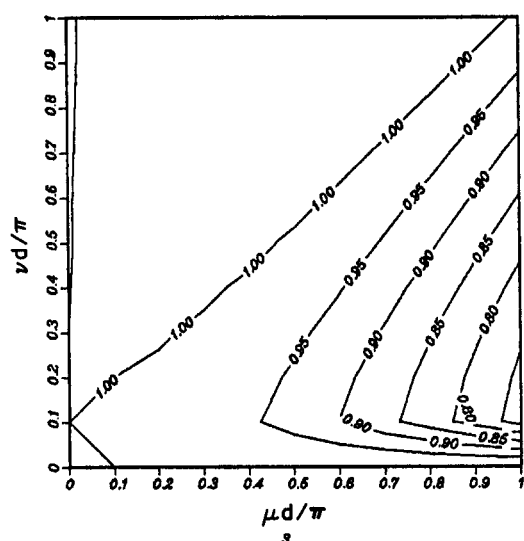
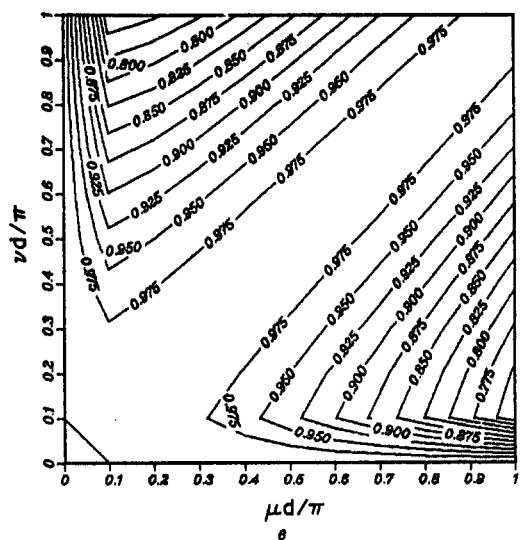
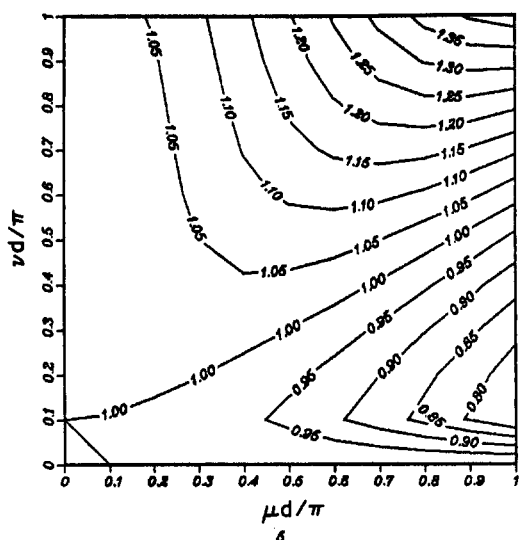


Fig. 8. Scheme B4.

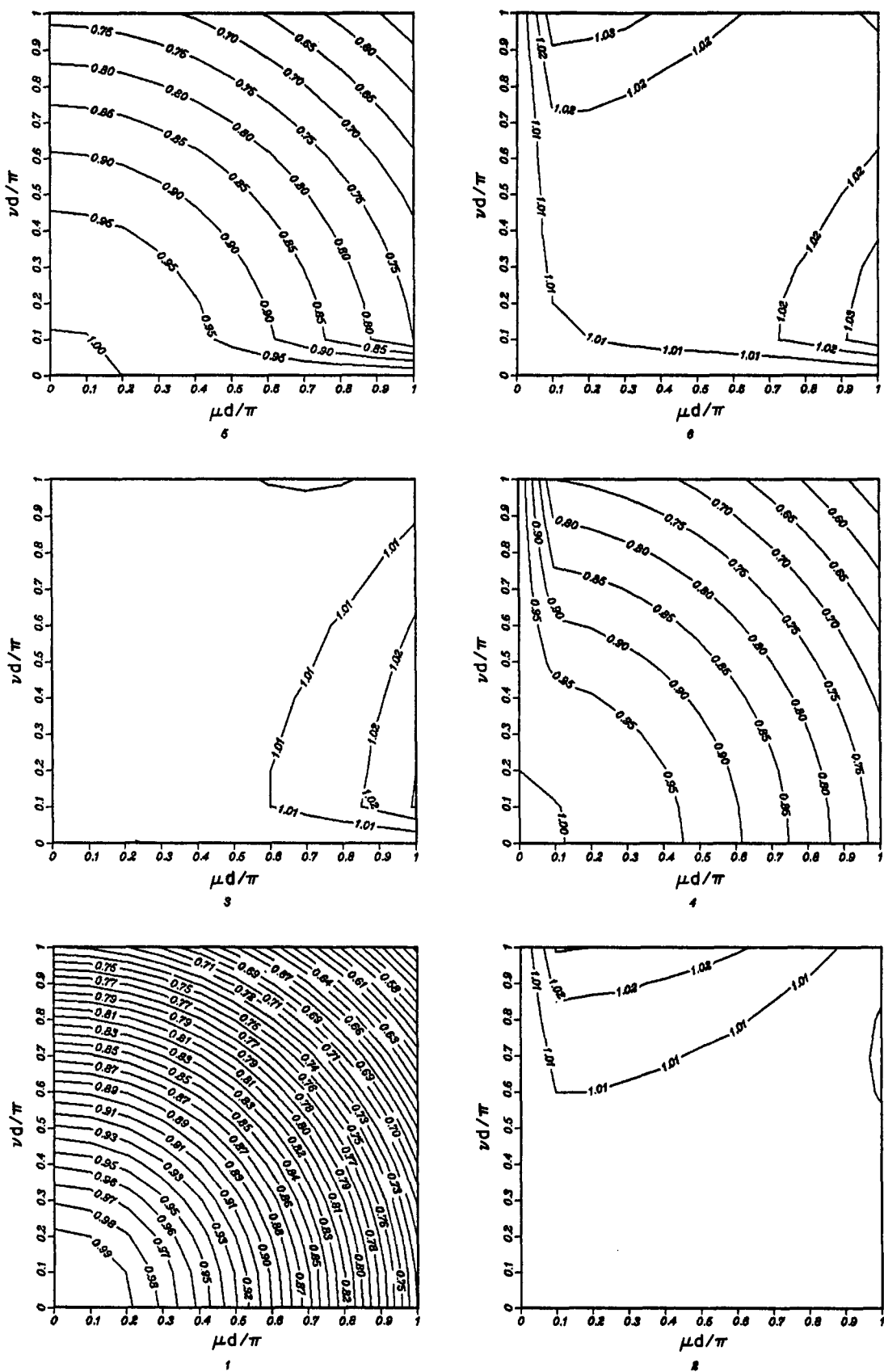


Fig. 9. Scheme C4.

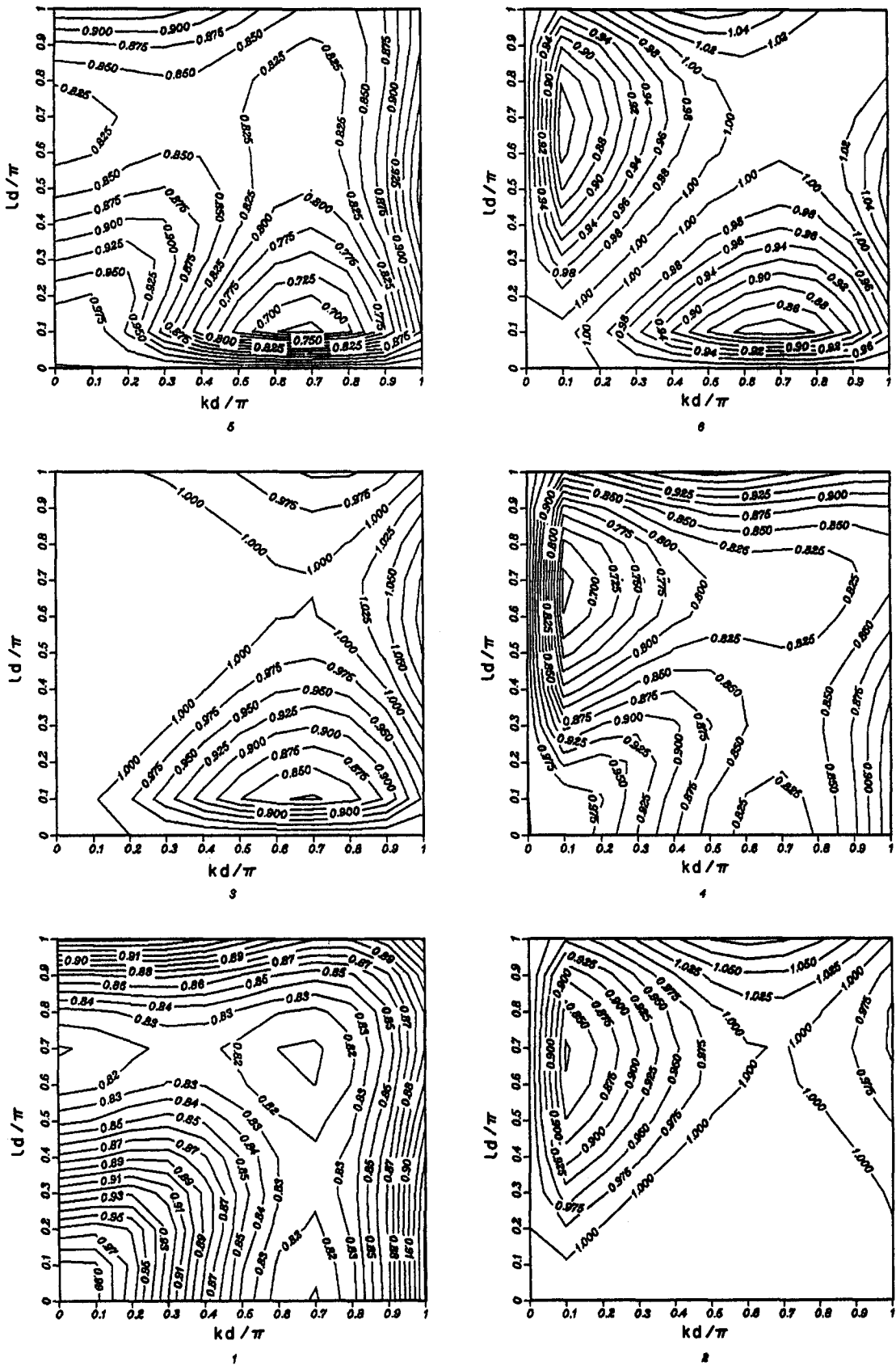


Fig. 10. Scheme D4.

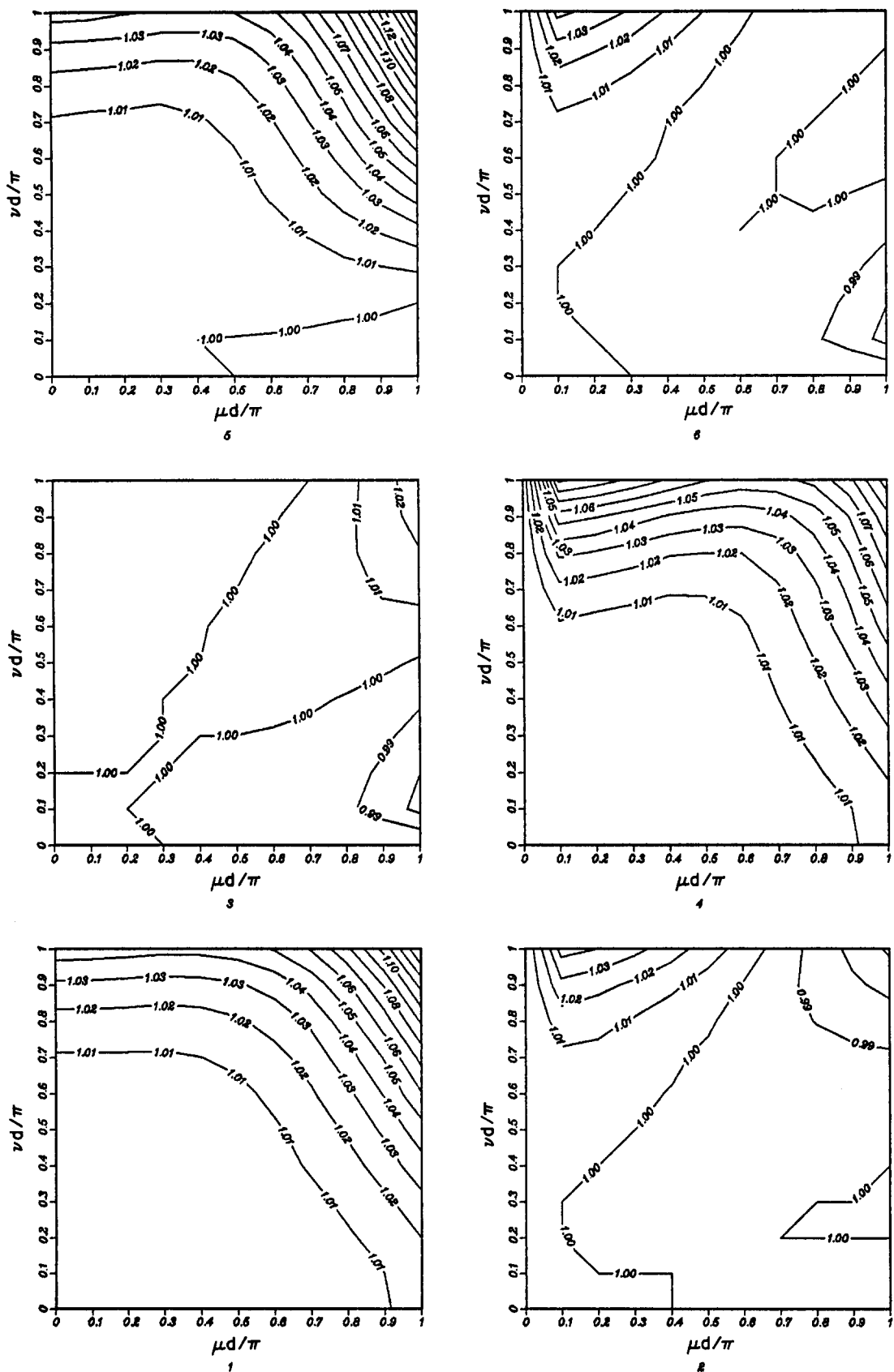


Fig. 11. Scheme FET.

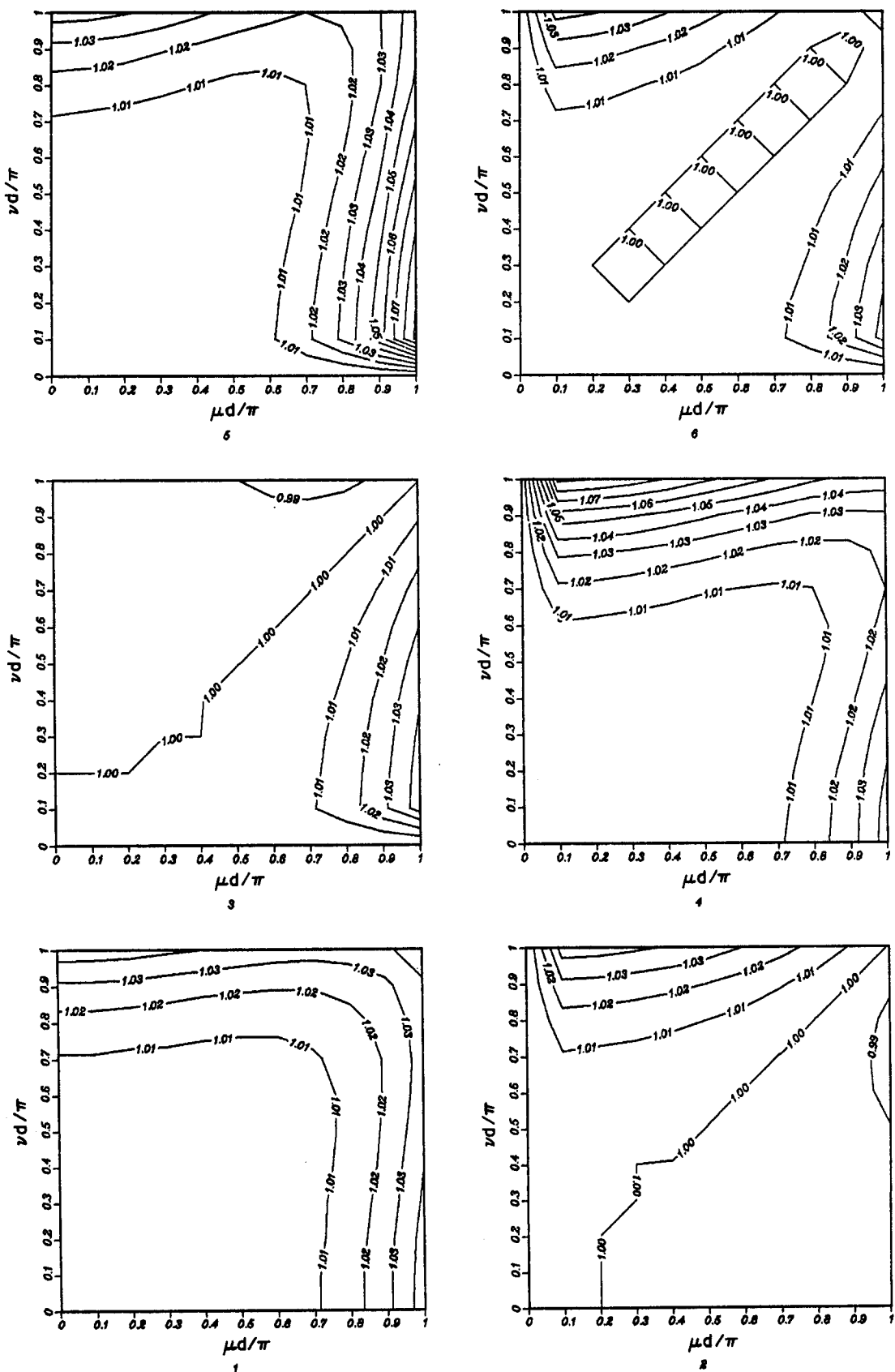
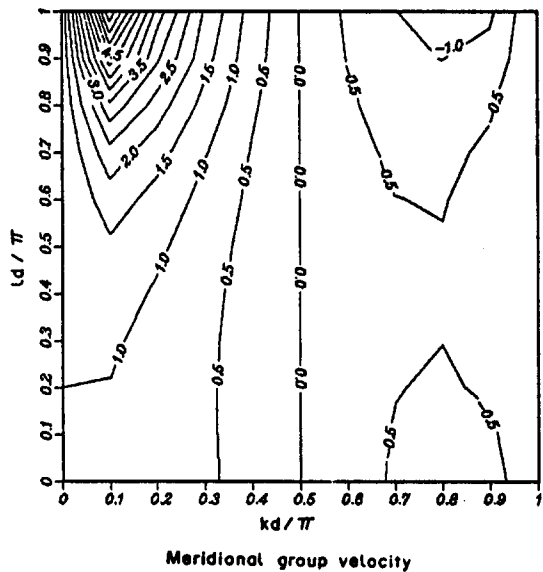
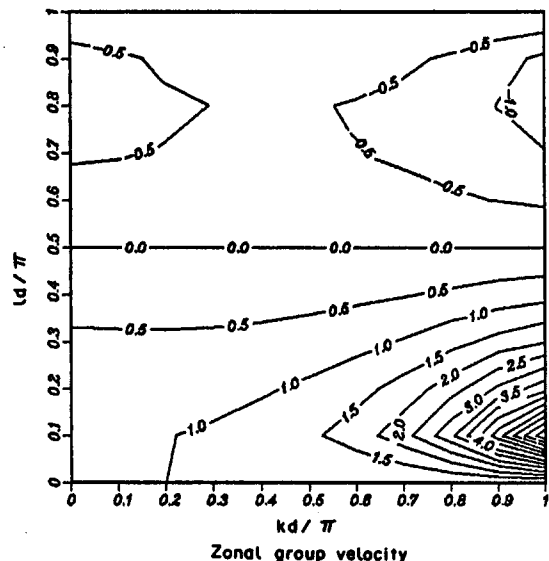


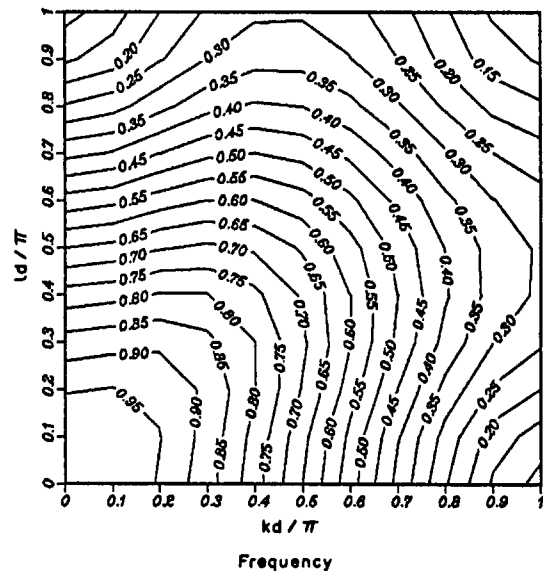
Fig. 12. Scheme FER.



Meridional group velocity

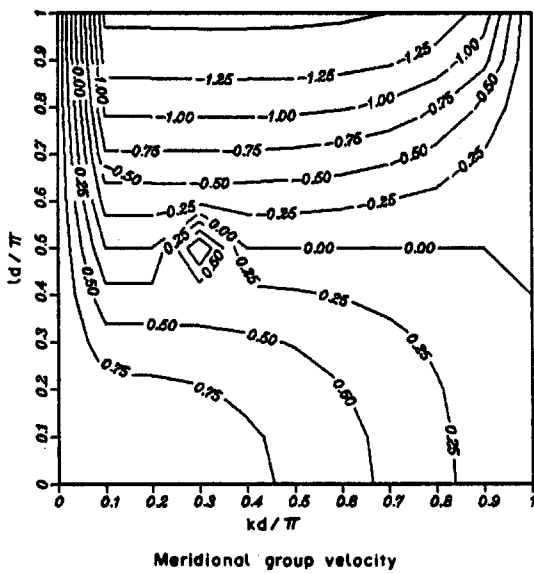


Zonal group velocity

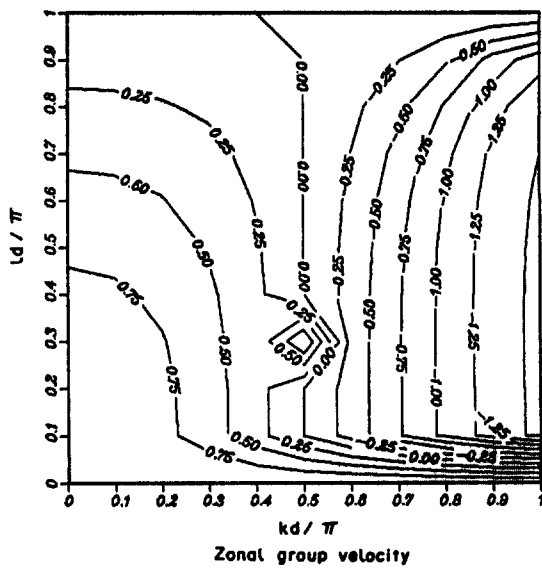


Frequency

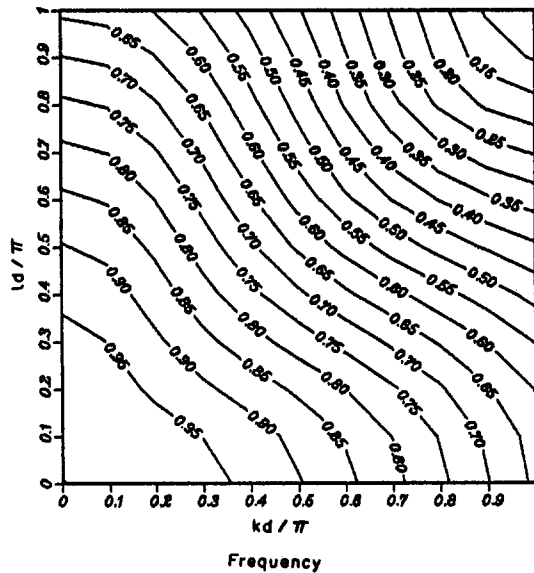
Fig. 13. Scheme A2.



Meridional group velocity



Zonal group velocity



Frequency

Fig. 14. Scheme B2.

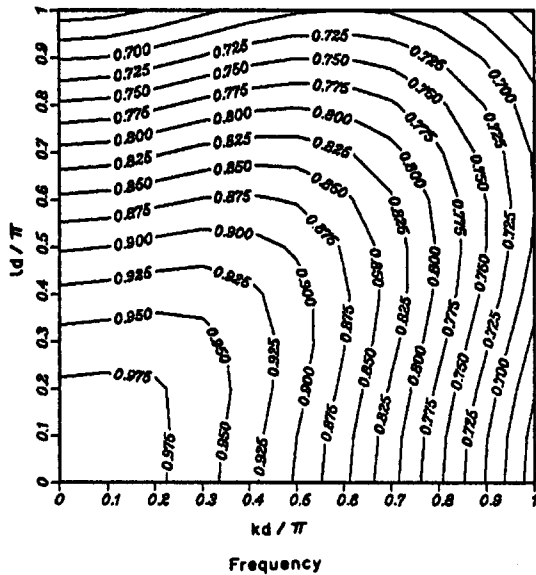
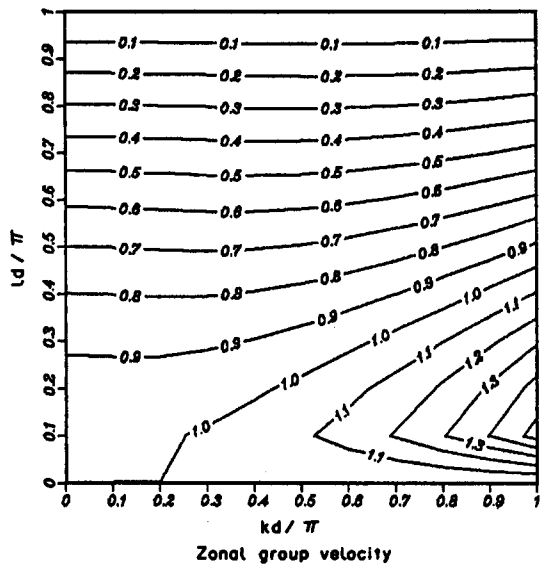
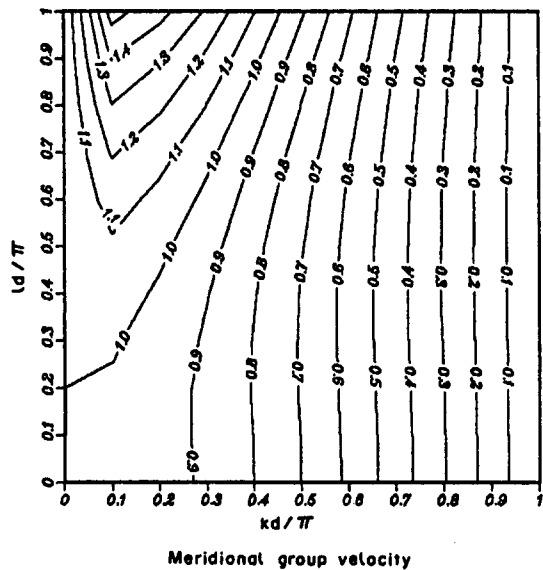
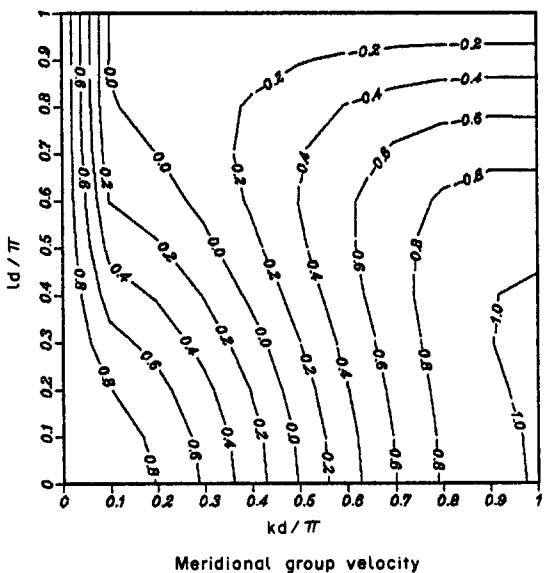
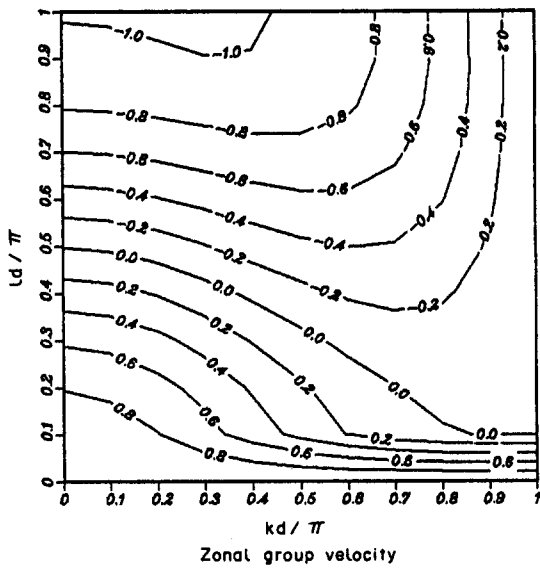


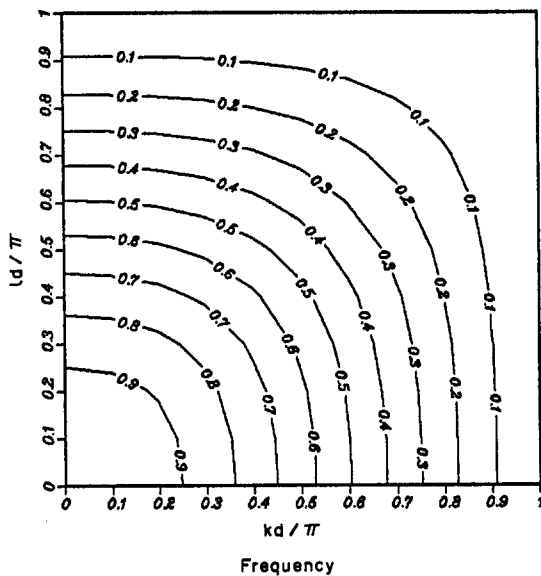
Fig. 15. Scheme C2.



Meridional group velocity



Zonal group velocity



Frequency

Fig. 16. Scheme D2.

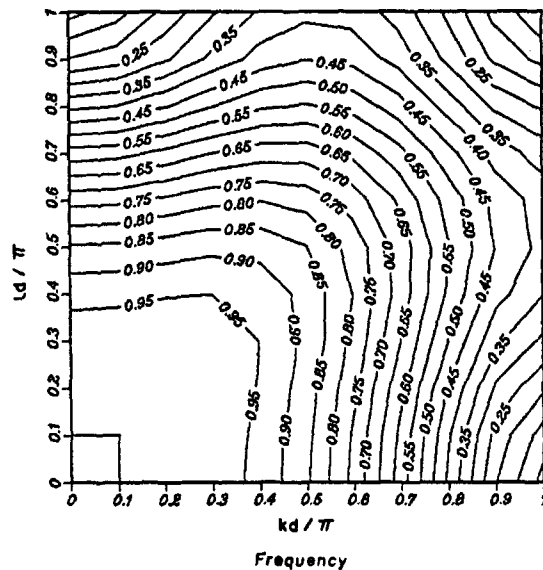
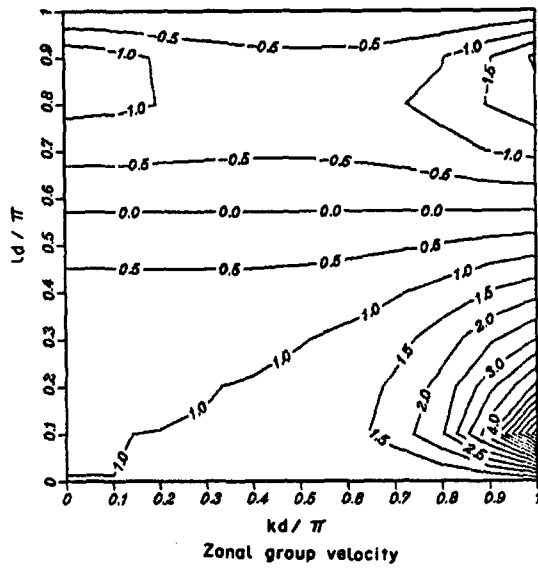
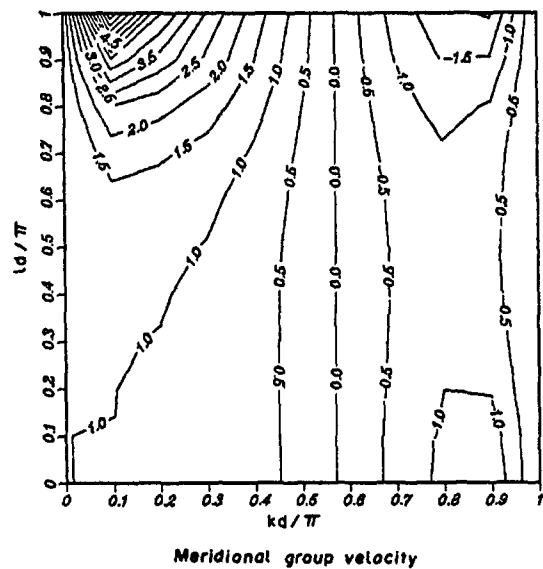
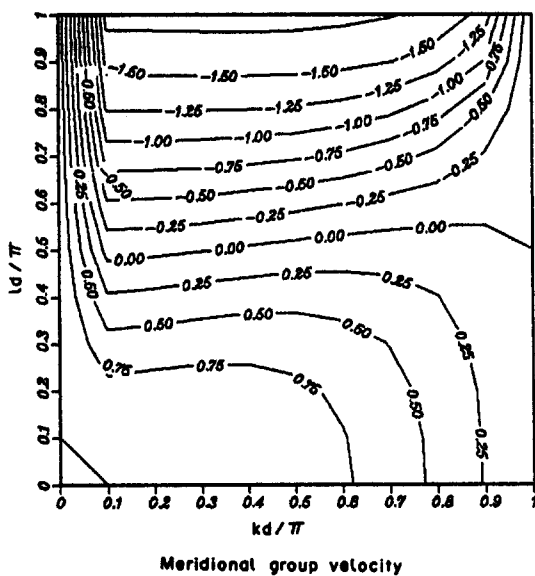
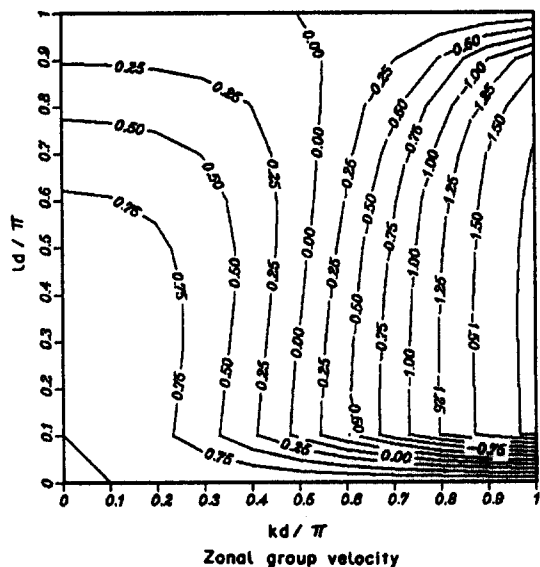


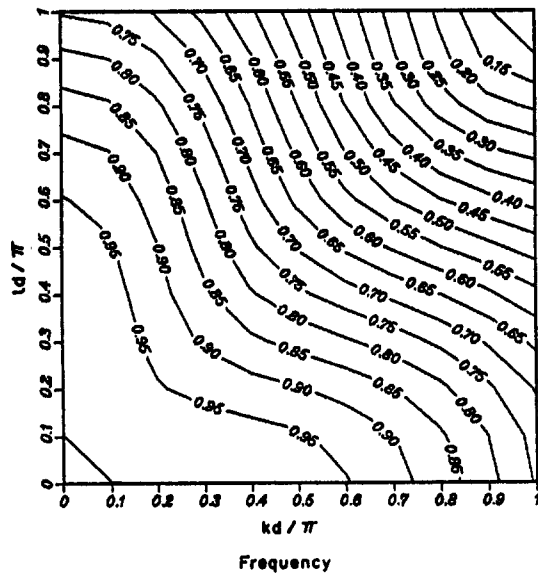
Fig. 17. Scheme A4.



Meridional group velocity



Zonal group velocity



Frequency

Fig. 18. Scheme B4.

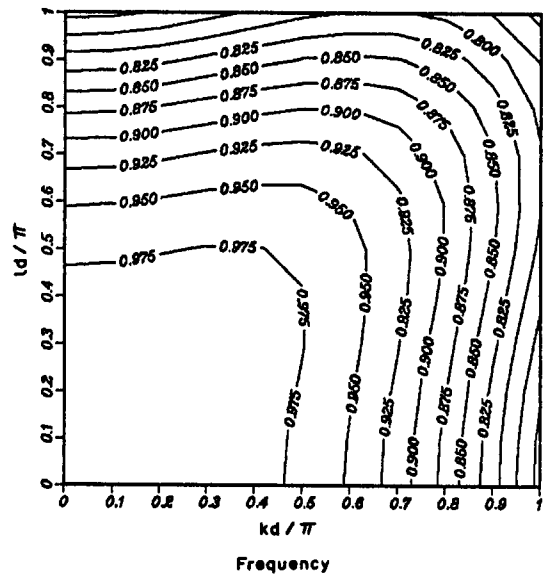
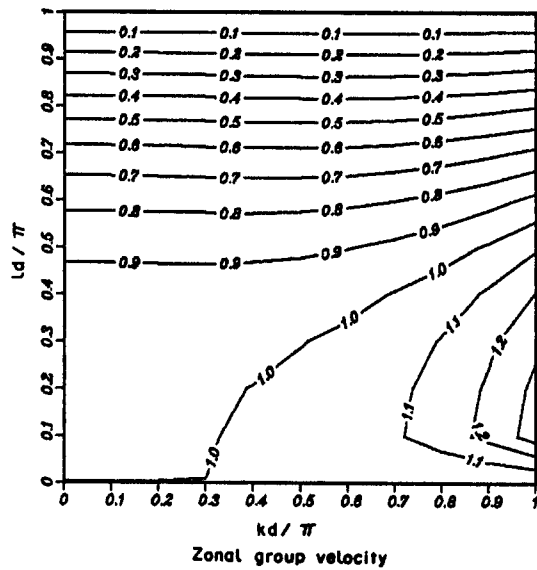
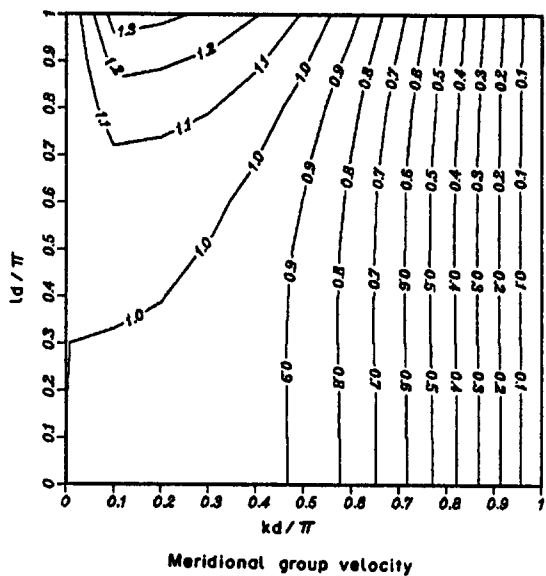
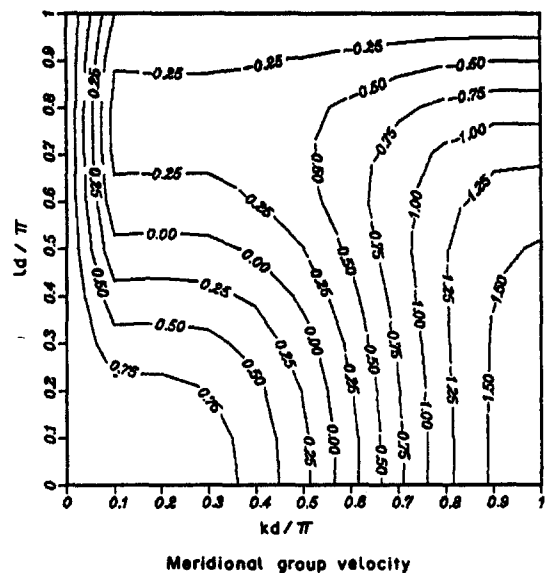
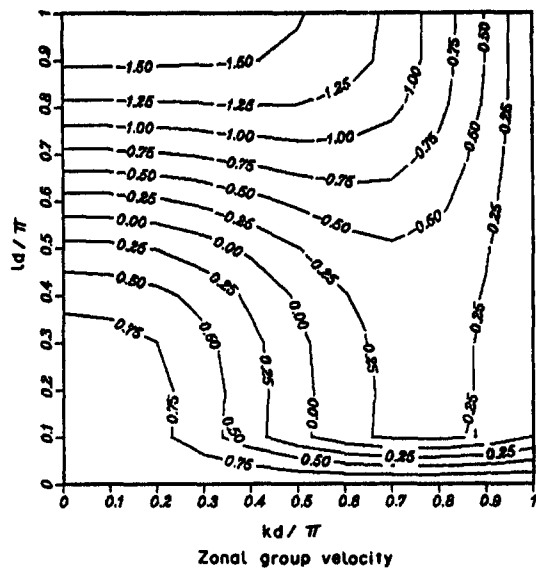


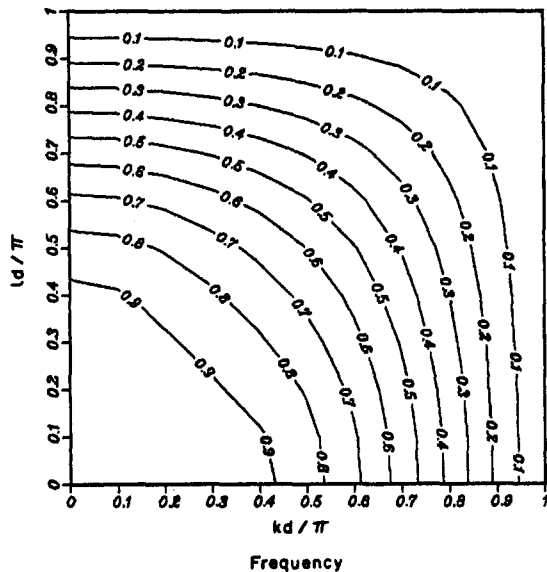
Fig. 19. Scheme C4.



Meridional group velocity

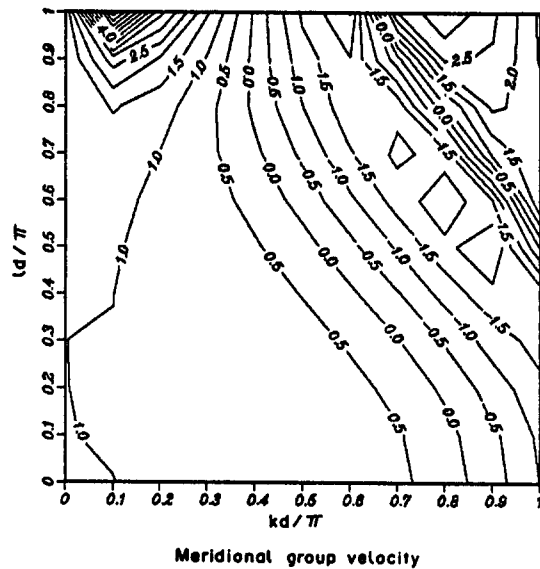


Zonal group velocity

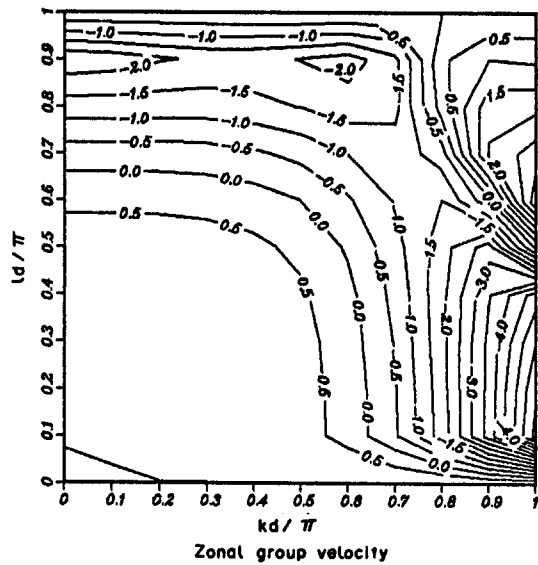


Frequency

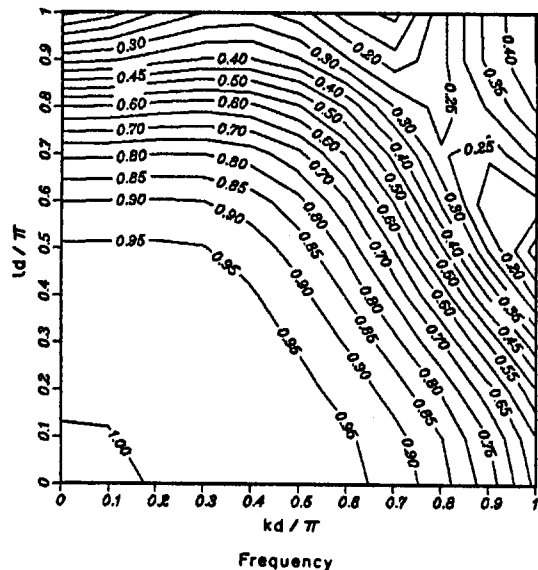
Fig. 20. Scheme D4.



Meridional group velocity

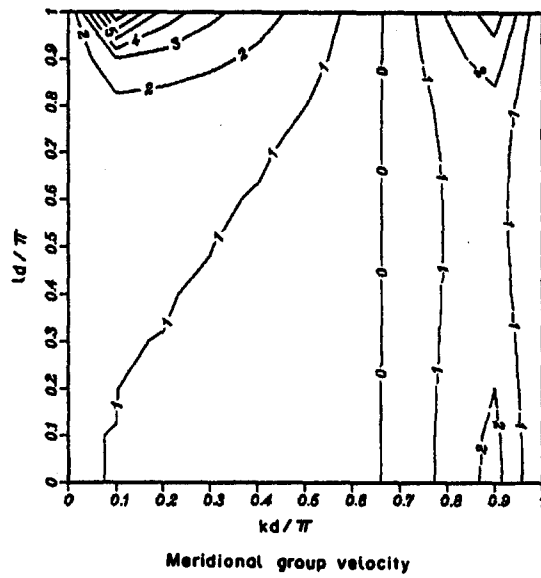


Zonal group velocity

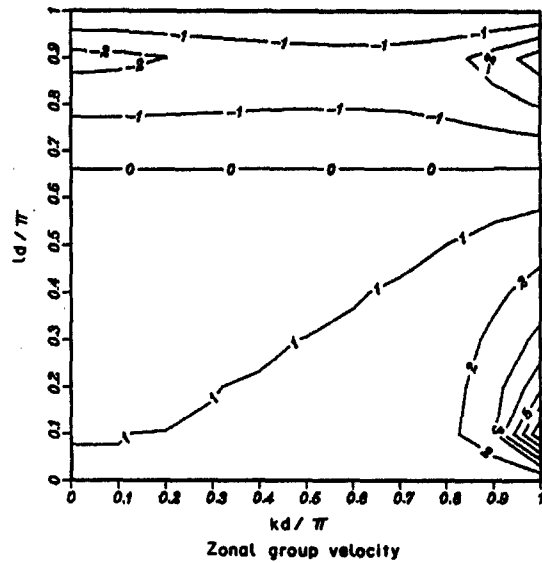


Frequency

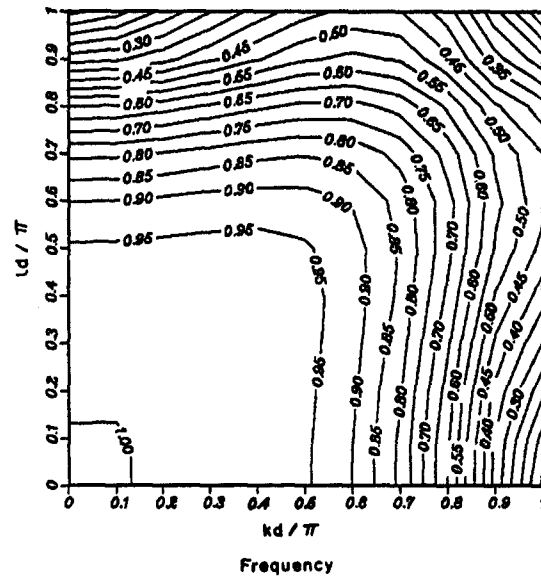
Fig. 21. Scheme FET.



Meridional group velocity



Zonal group velocity



Frequency

Fig. 22. Scheme FER.

filter coefficients of the rectangular finite element are closer to the exact one than any of the others, although the fourth-order C-scheme and the isosceles triangles are also good.

The zonal and meridional group velocities obtained by differentiation of equation (19) are given by

$$\frac{\partial v}{\partial k} = f \frac{\left[ \beta \frac{\partial \beta}{\partial k} + \lambda^2 \left( \gamma_1 \frac{\partial \gamma_1}{\partial k} + \gamma_2 \frac{\partial \gamma_2}{\partial k} \right) \right] \alpha - \frac{1}{2} \left[ \beta^2 + \lambda^2 (\gamma_1^2 + \gamma_2^2) \right] \frac{\partial \alpha}{\partial k}}{\alpha^2 \sqrt{\beta^2 + \lambda^2 (\gamma_1^2 + \gamma_2^2)}} \quad (20)$$

and

$$\frac{\partial v}{\partial l} = f \frac{\left[ \beta \frac{\partial \beta}{\partial l} + \lambda^2 \left( \gamma_1 \frac{\partial \gamma_1}{\partial l} + \gamma_2 \frac{\partial \gamma_2}{\partial l} \right) \right] \alpha - \frac{1}{2} \left[ \beta^2 + \lambda^2 (\gamma_1^2 + \gamma_2^2) \right] \frac{\partial \alpha}{\partial l}}{\alpha^2 \sqrt{\beta^2 + \lambda^2 (\gamma_1^2 + \gamma_2^2)}}. \quad (21)$$

The contours of the relative phase speed and relative zonal and meridional group velocities are plotted in Figs 13–22 for each of the schemes. It is easy to see that again the finite elements and the fourth-order C-scheme are superior to all others considered.

*Acknowledgement*—The first author would like to thank the NPS Foundation Research program for its support of this research.

## REFERENCES

1. A. L. Schoenstadt, A transfer function analysis of numerical schemes used to simulate geostrophic adjustment. *Mon. Weath. Rev.* **108**, 1248–1259 (1980).
2. C. G. Rossby, On the mutual adjustment of pressure and velocity distributions in certain simple current systems. *J. mar. Res.* **1**, 15–28, 239–263 (1937/38).
3. A. Cahn, An investigation of the free oscillations of a simple current system. *J. Met.* **2**, 113–119 (1945).
4. F. Winninghoff, On the adjustment toward a geostrophic balance in a simple primitive equation model with application to the problem on initialization and objective analysis. Ph.D. Dissertation, UCLA, Los Angeles, Calif. (1968).
5. W. Blumen, Geostrophic adjustment. *Rev. Geophys. Space Phys.* **10**, 485–528 (1972).
6. A. Arakawa and V. R. Lamb, Computational design of the basic dynamical processes of the UCLA General Circulation Model. In *Methods of Computational Physics*, Vol. 17, pp. 173–265. Academic Press, New York (1977).
7. A. L. Schoenstadt, The effect of spatial discretization on the steady-state and transient solutions of a dispersive wave equation. *J. comput. Phys.* **23**, 364–379 (1977).
8. B. Neta and I. M. Navon, The analysis of the Turkel-Zwas scheme for the shallow-water equations. Submitted for publication.
9. A. C. Hearn (Ed.), *REDUCE User's Manual*. Rand Corp., Santa Monica, Calif. (1983).
10. W. Washington, A note on the adjustment towards geostrophic equilibrium in a simple fluid system. *Tellus* **16**, 530–534 (1964).
11. B. Neta and R. T. Williams, Stability and phase speed for various finite element formulations of the advection equation. *Comput. Fluids* **14**, 393–410 (1986).
12. B. Neta, R. T. Williams and D. E. Hinsman, Studies in a shallow water fluid model with topography. In *Numerical Mathematics and Applications* (Edited by R. Vichnevetsky and J. Vignes), pp. 347–354. Elsevier, New York (1986).